



## Hydrogel biochar composite for arsenic removal from wastewater

M.L. Sanyang<sup>a</sup>, Wan Azlina Wan Abd Karim Ghani<sup>a,\*</sup>, Azni Idris<sup>a</sup>,  
Mansor Bin Ahmad<sup>b</sup>

<sup>a</sup>Department of Chemical and Environmental Engineering, Universiti Putra Malaysia, Serdang 43400, Selangor, Malaysia, Tel. +601128244787; email: [sanyang.abuhamza@gmail.com](mailto:sanyang.abuhamza@gmail.com) (M.L. Sanyang), Tel. +603 89466287; email: [wanz@upm.edu.my](mailto:wanz@upm.edu.my) (W.A.W.A.K. Ghani), Tel. +603 89466302; email: [azni@upm.edu.my](mailto:azni@upm.edu.my) (A. Idris)

<sup>b</sup>Department of Chemistry, Universiti Putra Malaysia, 43400 UPM Serdang, Selangor, Malaysia, Tel. +603 89466775/93; email: [mansorahmad@upm.edu.my](mailto:mansorahmad@upm.edu.my)

Received 16 March 2014; Accepted 6 November 2014

---

### ABSTRACT

Arsenic contaminated water is an environmental issue due to their toxicity. Acute arsenic poisoning has claimed the lives of many and causes adverse health risk to millions of people in several countries such as Bangladesh, India, and China. Effective removal of this contaminant can be obtained by adsorbing them onto low-cost adsorbents. In this study, hydrogel-biochar composite (HBC-RH) was successfully synthesized by embedding rice husk biochar into poly(acrylamide) hydrogel with N,N'-methylenebisacrylamide (MBA) as crosslinker. The synthesized HBC-RHs were characterized and utilized for the removal of arsenic from wastewater. The experimental parameters that influence the sorption process were investigated. The results obtained revealed that the effective removal of arsenic was found to be dependent on solution pH, sorbent dosage, initial contaminant concentration, and contact time. HBC-RH maximum monolayer sorption capacity for arsenic was 28.32 mg g<sup>-1</sup> and the experimental data suggested that the arsenic sorption was best fitted by pseudo-second-order kinetic mode. Above all, HBC-RH can easily be separated from aqueous solution after accomplishing its mission, avoiding separation complications faced by powder adsorbents in aqueous media.

*Keywords:* Arsenic; Wastewater; Hydrogel; Biochar; Isotherm; Kinetics

---

### 1. Introduction

Arsenic like all other heavy metals is non-biodegradable. They are discharged through numerous natural processes [1] and via range of anthropogenic activities such as mining, non-ferrous smelting, petroleum refining, combustion of fossil fuel in power plants, and the use of pesticides and herbicides containing arsenic [2]. Arsenic exists in many oxidation

states like -3, 0, +3, and +5. However, in natural waters it exists as oxyanions of trivalent arsenite As (III) or pentavalent arsenate As (V) [1]. In 2003, the World Health Organization set the arsenic maximum contamination level at 0.01 mg L<sup>-1</sup> [3]. Therefore, consumption of arsenic contaminated water with concentration beyond the acceptable standard leads to several health complications. The toxicity of arsenic is a complex phenomenon and mainly categorized into acute and sub-acute types [4]. Acute arsenic poisoning is due to long-term exposure to arsenic in drinking

---

\*Corresponding author.

water which eventually leads to cancer of the bladder, lungs, skins, kidney, nasal passages, liver, and prostate. Non-cancer effects of ingesting arsenic include cardiovascular, pulmonary, immunological, neurological, and endocrine (e.g. diabetes) effects [5]. The primary symptoms of sub-acute arsenic poisoning include burning and dryness of the mouth and throat, dysphasia, colicky abnormal pain, projectile vomiting, profuse diarrhea, and hematuria [4]. Hopenhayn-Rich et al. [6] stated that most probably, arsenic is the contaminant that induces the highest risk of morbidity and mortality worldwide, due to the number of people exposed to its toxicity.

There are numerous arsenic contaminated water treatment techniques such as adsorption, ion exchange, chemical precipitation, coagulation, ultra filtration, membrane filtration, solvent extraction, biological systems, reverse osmosis, photo-catalytic degradation, electrolytic processes, and oxidation with ozone/hydrogen peroxide [7–12]. However, adsorption removal method proves to be highly efficient and meritorious when compared with other conventional techniques in terms of simplicity and flexibility of design, ease of operation, and initial cost [13]. The threats generated from arsenic contaminated water can be averted by adsorption technique using low-cost adsorbents. Activated carbon has been the most popular employed adsorbent for the removal of most heavy metal ions from water/wastewater. However, it remains as an expensive adsorbent, limiting its application. Many other adsorbents have been investigated for the adsorption of arsenic from aqueous solutions [14–19] but all these adsorbents demonstrated some advantages as well as disadvantages regarding their removal performance, cost-effectiveness, and availability. Moreover, most of these adsorbents (including powdered activated carbon or biochar) are not readily separated from aqueous media after accomplishing their mission of removing contaminants. Due to the forth mentioned succinct limitations, there is an intensive research worldwide to develop low-cost, easy handled and highly efficient adsorbents from agricultural waste for arsenic removal from wastewater.

Rice husk is a potential adsorbent utilized for the removal of numerous heavy metals. Rice husk is 20% of the whole rice and contains about 20% silica [20]. Malaysia produces about 408,000 metric tons of rice husk each year [21]. The amount of rice husk available annually is far in excess for any domestic uses, thus, has led to disposal problems. Thermal conversion (i.e. pyrolysis) of raw rice husk to biochar provides a better environmental friendly waste management technique when compared to the conventional method of open burning which causes severe atmospheric

pollution and subsequently contributes to global climate warming. Whereas, rice husk biochar (RHB) can be utilized as a low-cost adsorbent for the removal of contaminants from aqueous solutions. However, the low adsorption capacity of RHB for the removal of heavy metals warrant the synthesis of a hydrogel modified biochar hydrogel-biochar composite (HBC-RH) sorbent. A neutral hydrogel which is cheap, easily handled, and readily available for biochar composite synthesis was utilized in this investigation. This modification can increase the surface sorption sites of the resulting HBC-RH by adding more surface functional groups, which can have dominant control on the sorption of arsenic from aqueous media.

Hydrogels are potential sorbents with crosslinked polymeric networks and contains hydrophilic groups that could be used as complexing agents for the removal of toxic metal ions from aqueous solutions [22–26]. Recently, hydrogels have attracted more attention due to its high adsorption capacity, easy loading, and separation from aqueous solutions. In this study, RHB were embedded into acrylamide-hydrogel (AAM-hydrogel) matrix (forming a hydrogel composite material) to overcome the limitations of pure polymeric hydrogels such as poor gel strength and stability as well as to further increase its sorption capacity. The synthesized hydrogel composite (HBC-RH) has advantages over empty AAM-hydrogel, due to its improved hydrophilicity and favorable functional groups. The presence of large number of functional ionized carboxyl group as well as hydroxyl and amino groups in the HBC-RH is expected to significantly improve arsenic removal from the wastewater.

The primary aim of this study is to develop an environmental friendly adsorbent, and to investigate its potential for the effective removal of arsenic from aqueous media. The main parameters that influence the sorption of arsenic from aqueous media will also be evaluated.

## 2. Materials and methods

### 2.1. Materials

Acrylamide (AAM) was used as monomer,  $N,N'$ -methylenebisacrylamide (MBA) as crosslinker, and ammonium persulfate (APS) as initiator. Hydrochloric acid and sodium hydroxide were used to adjust the pH of sample solutions. All the forth-mentioned chemicals are SIGMA products and purchased from Evergreen engineering and resources (Malaysia). The RHB used was obtained from Universiti Putra Malaysia gasification and pyrolysis house at the faculty of engineering.

## 2.2. Methods

### 2.2.1. Preparation of arsenic solution

The procedure for arsenic stock solution preparation was adopted from Chutia et al. [27]. The arsenic stock solution ( $1,000 \text{ mg L}^{-1}$ ) was prepared by dissolving sodium arsenate heptahydrate ( $\text{Na}_2\text{HAsO}_4 \cdot 7\text{H}_2\text{O}$ ) (98.5%, Sigma) in deionized (DI) water. This stock solution is diluted accordingly to prepare fresh arsenic solutions for each study. All reagents and chemicals used were of analytical grade or as mentioned.

### 2.2.2. HBC-RH synthesis

The preparation of hydrogel-rice husk derived biochar composite (denoted as HBC-RH) was in accordance with the procedure used by Karakoyun et al. [28]. Briefly, to synthesize HBC-RH sorbent, 1.0 g of AAm was dissolved in 1.0 mL of water. 0.6 g of RHB and 0.001 g of MBA were added to the AAm solution. After thorough mixing, 0.2 mL of 0.1 g aqueous solution of APS was added to initiate the polymerization. The hydrogel-biochar precursor solution was immediately placed into polyvinyl chloride (PVC) straws of 3 mm diameter and placed in an oven at  $40^\circ\text{C}$ . The HBC-RH was placed in the oven to speed up the polymerization and crosslinking process and to avoid the settling of biochar at the bottom of the PVC straws. The PVC straws containing HBC-RHs were removed from the oven after 30 mins and left for 24 h at room temperature ( $30^\circ\text{C}$ ) to ensure complete polymerization and crosslinking. HBC-RH was taken from the straws, cut to desired sizes, and washed several times with distilled water to remove all unreacted monomers and low molecular weight polymeric matter from the hydrogel. The washed HBC-RH was first dried in air before drying in a vacuum oven at  $40^\circ\text{C}$  for 24 h and then stored in a desiccator until used. Three different HBC-RH were synthesized, varying concentration of MBA crosslinker (0.1, 0.01, and 0.001 g of MBA) while all other parameters remain unchanged.

### 2.2.3. Characterization of hydrogel- biochar composites

**2.2.3.1. Swelling behavior.** The HBC-RHs were placed in beakers of distilled water to determine their swelling behaviors. The weight increases were measured at room temperature by periodically removing the hydrogel materials and weighing them. The following Eq. (1) was used to calculate the swelling ratio:

$$\text{Swelling ratio} = \frac{W_{\text{swollen}} - W_{\text{dry}}}{W_{\text{dry}}} \times 100 \quad (1)$$

The graph of percent swelling degree (S%) of the hydrogel composite materials against time in DI water were plotted to examine the trends. The highest swollen HBC-RH was utilized for characterization and sorption studies.

**2.2.3.2. Fourier transform infrared spectroscopy.** The Fourier transform infrared spectroscopy (FTIR) analysis was performed for HBC-RH by FTIR Perkin Elmer Spectro 100 series (USA). This was to identify the functional groups that exist in HBC-RH. The samples were grinded with potassium bromide (KBr) and pressed at pressure of 40kN to generate transparent thin pellets. The analyses were done at maximum resolution of  $4 \text{ cm}^{-1}$  in the wavelength range  $4,000\text{--}650 \text{ cm}^{-1}$ .

### 2.2.4. Effect of pH on arsenic removal

The pH of the solution is an essential parameter that affects the adsorption process. Thus, the pH study was conducted by varying adsorbate solution pH from 4 to 10 and initial arsenic concentration was  $3 \text{ mg L}^{-1}$ . The pH of the solution was adjusted by adding 0.1 M HCl and NaOH solution. The adsorbate solution (300 mL) was equilibrated by 0.3 g HBC-RH and the samples were agitated for 2 d. All other experiments in this study were conducted at the optimum pH obtained to achieve maximum arsenic removal.

### 2.2.5. Effect of adsorbent dosage on arsenic removal

Adsorbent dosage is among the adsorption process parameters that greatly influence the removal of adsorbate from aqueous solutions [29]. Thus, the quantity of adsorbent was varied from 0.167 to  $16.67 \text{ g L}^{-1}$  ( $0.05\text{--}5 \text{ g}/300 \text{ mL}$ ) while initial arsenic concentration and pH remained constant.

### 2.2.6. Effect of initial concentration on arsenic removal

Batch adsorption study of arsenic was conducted using conical flasks filled with 300 mL of each solution over different arsenic concentrations ( $1\text{--}150 \text{ mg L}^{-1}$ ). The pH of the solutions were adjusted by using 0.1 M HCl and NaOH.

0.3 g of HBC-RH were added into each solution and then placed in an incubator shaker to shake the solutions at 150 rpm and the operating temperature was  $28^\circ\text{C} (\pm 2^\circ\text{C})$ . The samples were agitated for complete 2 d to ensure that equilibrium was obtained. Thereafter, the adsorbents were separated from the

agitated samples. The filtered solutions were analyzed using ICP-MS.

### 2.2.7. Effect of contact time on arsenic removal

Batch kinetic study was done to determine the dynamic behavior of HBC-RH as an adsorbent for the removal of arsenic from aqueous solutions. In these kinetic studies, 300 mL of arsenic was shaken with HBC-RH (0.3 g) at constant temperature of 28°C ( $\pm 2^\circ\text{C}$ ) and the pH were set at optimum. Samples of 5 mL were carefully extracted from the solutions periodically (0.5–48 h). All extracted samples were analyzed using ICP-MS.

### 2.2.8. Calculation of metal uptake and removal percentage

The mass balance Eq. (2) was used to calculate the amount of arsenic adsorbed per adsorbent mass unit (arsenic uptake) [30].

$$q = \frac{(C_o - C)V}{M} \quad (2)$$

where  $q$  is the amount of arsenic adsorbed per adsorbent mass unit ( $\text{mg g}^{-1}$ ).  $C_o$  and  $C$  are the initial and final arsenic concentration ( $\text{mg L}^{-1}$ ) in the solution.  $V$  (L), and  $M$  (g) are the volume of solutions and mass of adsorbents, respectively.

The arsenic removal percentage was determined by (3):

$$\text{Metal removal \%} = \frac{(C_o - C_e)}{C_o} \times 100 \quad (3)$$

where  $C_e$  is the concentration of arsenic in the solution at equilibrium.

### 2.2.9. Isotherm modeling studies

Langmuir and Freundlich isotherm were employed to simulate the arsenic sorption onto the HBC-RH. The Langmuir model in Eq. (4) assumes monolayer adsorption onto a homogeneous surface with no interactions between the adsorbed molecules.

$$\frac{C_e}{q_e} = \frac{1}{q_{\max} K_L} + \frac{C_e}{q_{\max}} \quad (4)$$

where  $C_e$  is the equilibrium concentration of arsenic ( $\text{mg L}^{-1}$ ) whereas  $q_e$  and  $q_{\max}$  are the amount of

arsenic adsorbed onto the HBC-RH ( $\text{mg g}^{-1}$ ) and maximum amount of arsenic the HBC-RH can adsorb ( $\text{mg g}^{-1}$ ).  $K_L$  is the Langmuir adsorption equilibrium constant ( $\text{L mg}^{-1}$ ).

The Freundlich model (5) is an empirical equation which is often used to describe chemisorption onto heterogeneous surface.

$$\log q_e = \log K_F + \frac{1}{n} \log C_e \quad (5)$$

where  $K_F$  and  $n$  are the Freundlich adsorption equilibrium constant and adsorption intensity, respectively.

### 2.2.10. Kinetic modeling studies

Pseudo-first-order Eq. (6) and pseudo-second-order kinetic models Eq. (7) were used to analyze the adsorption rate of arsenic adsorption onto the HBC-RH.

$$\log(q_e - q_t) = \log q_e - \frac{k_1}{2.303} t \quad (6)$$

$$\frac{t}{q_t} = \frac{1}{k_2 q_e^2} + \frac{1}{q_e} t \quad (7)$$

where  $k_2 q_e^2 (V_o)$  is the initial sorption rate,  $q_t$  and  $q_e$  are the amount of arsenic that is adsorbed at time  $t$  and at equilibrium, respectively.  $k_1$  and  $k_2$  are the first-order and second-order adsorption rate constants, respectively. The first-order and second-order models describe the kinetics of the solid-solution system based on mononuclear and binuclear adsorption, respectively, with respect to the sorbent capacity [31].

## 3. Results and discussion

### 3.1. HBC-RH synthesis

In this present study, the polymerization reaction of acrylamide (AAm) with N,N'-methylenebisacrylamide (MBA) in the presence of rice husk biochar (RH-Biochar) was obtained by introducing an initiator agent called APS. The introduction of APS into the precursor solution initiates the polymerization and crosslinking process simultaneously.

Different quantities of RHB were tried (0.06–1 g) during HBC-RH synthesis. However, the most appropriate amount of RH-Biochar that could be incorporated inside the hydrogel matrices was 0.6 g (biochar) in 1 mL of distilled water. Therefore, 0.6 g of RHB was utilized for all the subsequent HBC-RH synthesis.

It was observed that this combination yielded the best homogeneous HBC-RH.

### 3.2. HBC-RH swelling behavior

Water diffused into HBC-RH network chains as the HBC-RH was brought in contact with distilled water. This mass transfer of water into the dried HBC-RH rendered it swollen. The swelling of hydrogel materials are triggered by water diffusion into their interior, resulting in large-scale segmental motion which increases the distance between neighboring chains [32]. The dry HBC-RH appears glassy and very hard but soft and spongy when swollen as shown in Fig. 1.

The swelling ratio percent ( $S\%$ ) graph depicted in Fig. 2 initially increased drastically which was later followed by a slow increase until it finally level off at 1,008%. The  $S\%$  value where the graph level off is known as the equilibrium swelling percent ( $S_{eq}\%$ ). The  $S_{eq}\%$  was obtained after 24 h of HBC-RH and water contact time. The contact time was extended to 48 h to determine any further swelling but no significant increase was realized. The high swelling capacity of HBC-RH can be attributed to the presence of hydrophilic groups (i.e. amino, carboxyl, and hydroxyl groups) in the composite material as manifested by the FTIR spectrum of HBC-RH. Ozayet al. [33] reported that hydrophilic functional groups such as  $-\text{OH}$ ,  $-\text{COOH}$ ,  $-\text{NH}_2$ ,  $-\text{CONH}_2$ , and  $-\text{SO}_3\text{H}$  in hydrogel networks grant them the ability to absorb large quantity of water and consequently swell.

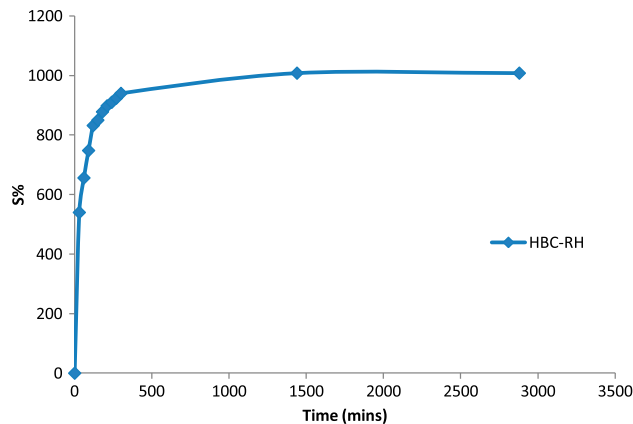


Fig. 2. Swelling ratio percent ( $S\%$ ) of HBC-RH.

### 3.3. Effect of crosslinker concentration on HBC swelling behavior

HBC-RH was effectively synthesized with MBA as crosslinker. Crosslinks prevent dissolution of the HBC-RH network chains when immersed in aqueous media. Even minute quantity of crosslinker plays a significant role in modifying the swelling and mechanical properties of hydrogels. To determine the effect of MBA crosslinker concentration on the swelling behavior of HBC-RH, three different MBA concentrations (0.1, 0.01, and 0.001 g MBA) were used while all other parameters remain unchanged.

Fig. 3 illustrates that  $S_{eq}\%$  increases from 472 to 1,008% as MBA concentration decreases from 0.1 to 0.001 g. This shows that the equilibrium swelling ratio percent was high at lower MBA concentration and

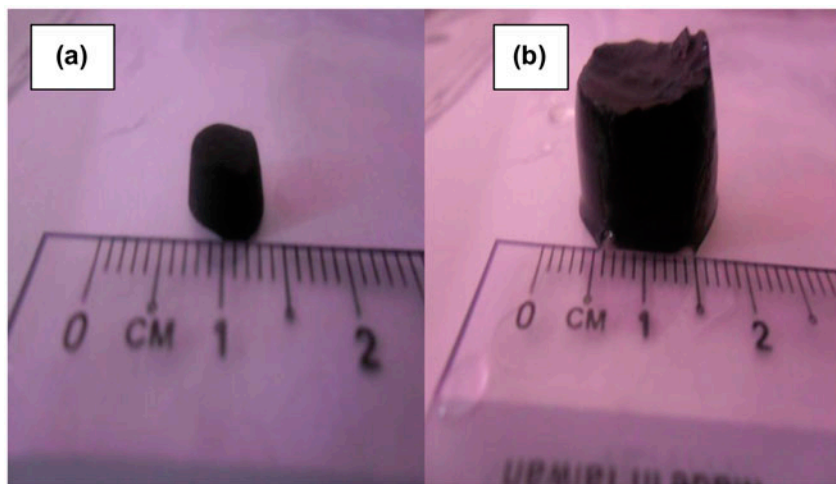


Fig. 1. Photographic image of (a) dry HBC-RH and (b) swollen HBC-RH.

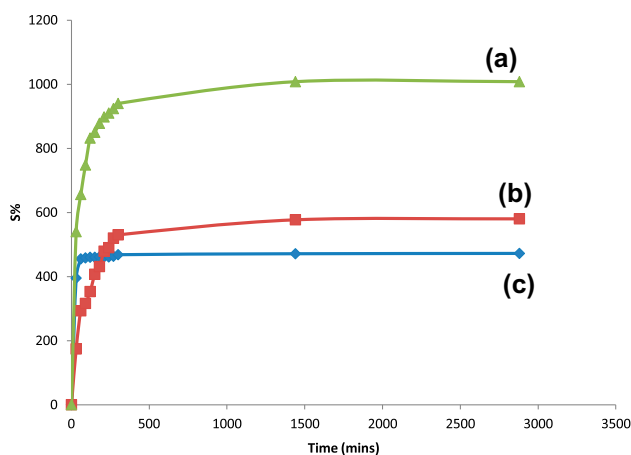


Fig. 3. Effect of MBA crosslinker concentration (a) 0.001 g, (b) 0.01 g, and (c) 0.1 g on HBC swelling ratio percent.

decreases with further addition of MBA crosslinker concentration. The influence of crosslinker concentration on hydrogel composite swelling phenomena can be elucidated based on the formation of network chains [34]. The HBC-RH with the lowest MBA content (HBC-3) has lesser crosslink density which permits large-scale mobility of network chains. As the MBA concentration in HBC-RH increases, it leads to an increase in the density of crosslinks per unit volume thereby suppressing the HBC-RH from fully swelling. These findings concur with the findings of numerous researchers [20,33,35,36]. The values of equilibrium water content percent (EWC %) were 82.5, 85.3, and 90.97% for 0.1, 0.01, and 0.001 g of MBA, respectively. The EWC% of HBC also increases as crosslinker concentration decrease and it drops as crosslinking density increases at higher MBA concentration.

#### 3.4. Functional groups of RHB, AAm-hydrogel, and HBC-RH

The FTIR spectra of RHB, AAm-hydrogel, and HBC-RH are shown in Fig. 4 to determine their prime functional groups. The crosslinked AAm-hydrogel spectrum exhibits the characteristic absorption peaks of polyacrylamide:  $3,214\text{ cm}^{-1}$  ( $-\text{OH}$  and  $\text{N}-\text{H}$  stretching),  $2,344\text{ cm}^{-1}$  (carboxylic group,  $-\text{COOH}$ ),  $1,628\text{ cm}^{-1}$  (carbonyl group of amide,  $\text{CONH}_2$ ), and  $834\text{ cm}^{-1}$  ( $\text{C}-\text{H}$ ) [22]. Comparing the spectrum of HBC-RH to that of AAm-hydrogel, the broad peak that appeared in the region of  $3,600\text{--}3,000\text{ cm}^{-1}$  corresponds to  $-\text{OH}$  stretching which overlapped with  $\text{N}-\text{H}$  groups showed an increase in intensity. The presence of strong absorption band at  $1,659\text{ cm}^{-1}$  in

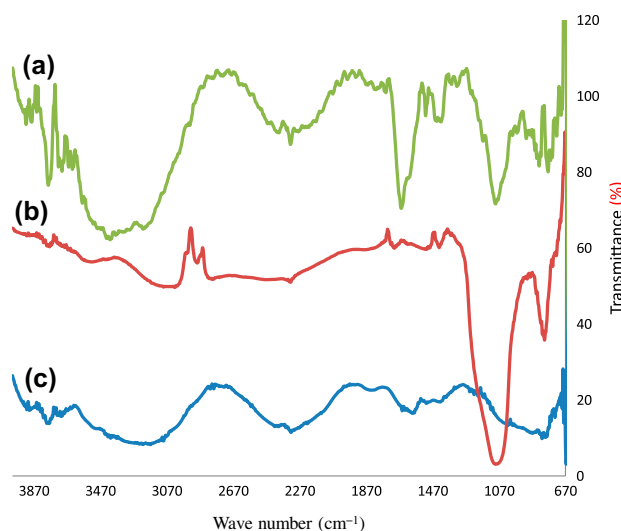


Fig. 4. Infrared spectrum of (a) HBC-RH, (b) AAm-hydrogel, and (c) RHB.

the HBC-RH spectrum, confirms the existence of carboxylate anion ( $\text{COO}^-$ ), meanwhile this peak overlaps with amide  $\text{C}=\text{O}$  peak from AAm and MBA crosslinker units. The presence of more oxygen-containing functional groups in HBC-RH would generate a relatively more hydrophilic character in HBC-RH than AAm-hydrogel. In addition, the peak at  $1,090\text{ cm}^{-1}$  that appeared in HBC-RH was due to stretching vibration of ether ( $\text{C}-\text{O}$ ) groups but it is absent in the AAm-hydrogel spectrum. The dominant absorption peak for RHB appeared at  $1,116\text{ cm}^{-1}$  indicating the presence of inorganic compounds (i.e.  $\text{SiO}_2$ ). Thus, the peak at  $1,090\text{ cm}^{-1}$  in HBC-RH spectrum might be due to the incorporation of silica from RHB into AAm-hydrogel matrix forming  $\text{CH}_2\text{--O--Si}$  during the synthesis of HBC-RH. HBC-RH increase in hydrophilicity coupled with decrease in silica content provides it better sorption capacity over AAm-hydrogel and RHB alone.

#### 3.5. Effect of pH on arsenic removal

The sorption of arsenic from aqueous media was significantly influenced by varying the pH of the media from 4 to 10. The surface charge of HBC-RH and the degree of ionization and speciation of arsenic was greatly affected by the pH of the solution. The surface charge of sorbents can be positive or negative or even neutral depending on the pH of the solution [37].

Fig. 5 shows the effect of pH on the removal of arsenic by HBC-RH, AAm-hydrogel, and RHB. It was observed that the HBC-RH removal of arsenic

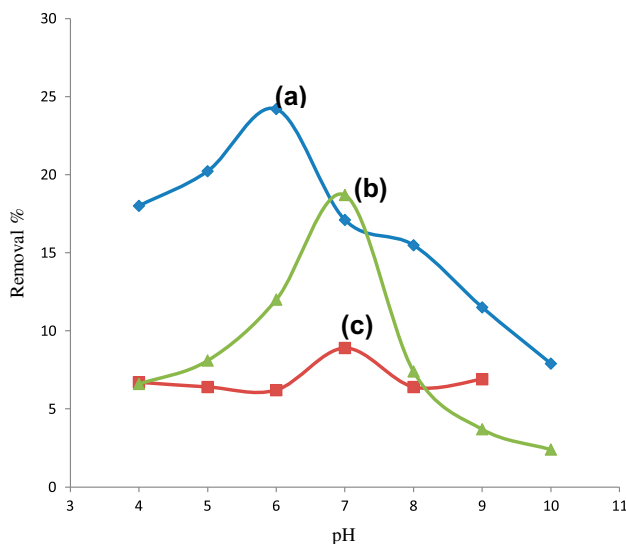


Fig. 5. Effect of pH on the sorption of arsenic using (a) HBC-RH, (b) AAm-hydrogel, and (c) RHB.

increases from pH 4 to 6, whereas it decreases beyond pH 6–10. The highest arsenic sorption onto HBC-RH ( $0.835 \text{ mg g}^{-1}$ ) was accomplished at pH 6. The ionizable functional groups, such as  $-\text{NH}_2$  and  $-\text{COO}^-$  on the surface of HBC-RH and AAm-hydrogel are protonated (at low pH) and the surface becomes positively charged. Thus, as pH value increases (pH 4–7) their removal capacity for arsenic also increases. This result concurs with the findings of Tiwari and Lee [38]. Their highest arsenate uptake occurred at pH 5.5 and then followed a significant decrease beyond pH 6. Chakraborty et al. [15] also obtained maximum arsenate adsorption onto calcined bauxite ore in a broad pH range of 4 to 7 and it continuously decreased afterwards.

The arsenic uptake of RHB at pH 7 was  $0.267 \text{ mg g}^{-1}$ . The low arsenic removal demonstrated by RHB in Fig. 5 was attributed to the large presence of  $\text{SiO}_2$  on the surface of RHB, which has a negative affinity to the sorption of metal ions. The potentiality of a sorbent to remove metal ions from aqueous solutions is significantly controlled by the number of available functional groups used for binding metals [39]. HBC-RH showed a better sorption capacity than AAm-hydrogel and RHB due to its high hydrophilic nature observed in Fig. 4. This high sorption ability of HBC-RH is connected to the presence of hydroxyl ( $-\text{OH}$ ), amine ( $-\text{NH}-$ ), and carboxyl ( $-\text{COO}^-$ ) groups which possesses strong affinity to metal ions.

The  $\text{pH}_{\text{ZPC}}$  (zero point charge) of sorbents also helps in comprehending the effect of pH on the sorption of both anionic and cationic metals in aqueous

media.  $\text{pH}_{\text{ZPC}}$  is the pH at which a neutral sorbent surface charge is achieved. Therefore, sorbents are positively charged when the solution pH is below the  $\text{pH}_{\text{ZPC}}$  value and vice versa [40]. The adsorption of anionic metal species is highly favorable at lower pH than the  $\text{pH}_{\text{ZPC}}$  of the sorbent. The sorbent surface charge is positive at pH less than the  $\text{pH}_{\text{ZPC}}$  due to the protonation of the surface active sites. Thus, it can be suggested that the high arsenic sorption at pH 6 was facilitated by the electrostatic attraction between the positively charged HBC-RH and the oxyanion species of arsenate. However, the observed decrease in arsenic removal (pH > 6) can be attributed to the increasing hydroxyl ions ( $\text{OH}^-$ ) in solution (at higher pH). The  $\text{OH}^-$  ions compete with the arsenic species for the available active sites. At  $\text{pH} > \text{pH}_{\text{ZPC}}$ , the HBC-RH surface charge becomes negative and causes repulsive effect which decreases the sorption of arsenic. This might be responsible for the steady decline of arsenic removal from pH 7 to 10 for all three sorbents. Furthermore, Manna and Ghosh [41] attributed the adsorption of arsenate at  $\text{pH} \leq 6$  to ligand or anion exchange phenomenon. Barakat and Sahiner [32] reported that arsenate can freely diffuse into the 3D network chains of hydrogel via electrostatic interactions between positively charged species in the hydrogels and the negatively charged arsenate ( $\text{H}_2\text{AsO}_4^-$ ) once the hydrogel is fully swollen. The dominant arsenate species at pH 5 to 6.5 is  $\text{H}_2\text{AsO}_4^-$ .

Besides HBC-RH high sorption capacity over RHB, it is readily dispersed in the solution and easily separated from the solution after adsorbing arsenic. This fact is visually illustrated in Fig. 6.

### 3.6 Effect of HBC-RH dosage on arsenic removal

Sorbent dosage plays essential role for the sorption of contaminants from aqueous media. It helps to determine the optimum sorbent–sorbate ratio for more effective and efficient sorption. In this study, HBC-RH doses were varied from  $0.167$  to  $16.67 \text{ g L}^{-1}$  ( $0.05$ – $5 \text{ g}/300 \text{ mL}$ ) while initial arsenic concentration ( $3 \text{ mg L}^{-1}$ ) and pH (6.0) remained unchanged.

The arsenic removal percent depicted in Fig. 7 increased as more HBC-RH doses were added to the solution. Increasing HBC-RH dosage from  $0.167$  to  $16.67 \text{ g L}^{-1}$  induces significant increase in arsenic removal from 18.35 to 93%. This increase was attributed to the high availability of favorable sorption sites on the sorbent surface. Chen et al. [42] reported that the removal percent of arsenate increased very rapidly with an increase in bone char concentration. He also



Fig. 6. Comparison between a sample solution with biochar and HBC-RH as sorbent (Left: Biochar in solution; Right: HBC-RH in solution).

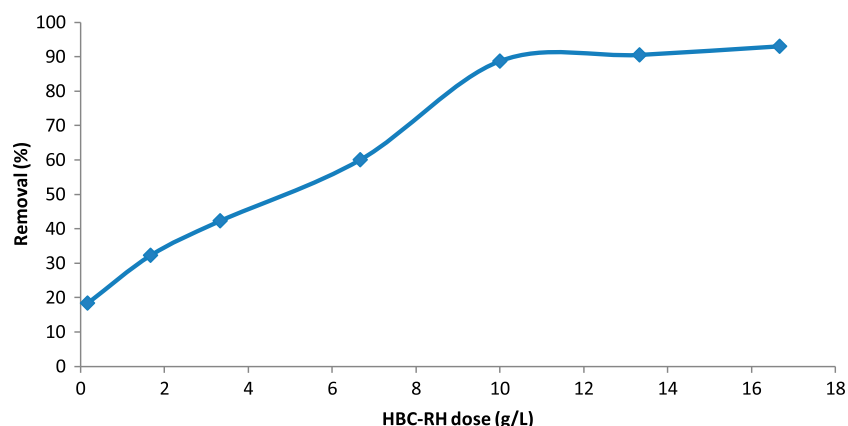


Fig. 7. Effect of HBC-RH dosage on the sorption of arsenic (Arsenic:  $3 \text{ mg L}^{-1}$ , pH 6, 48 h, and  $28^\circ\text{C}$ ).

suggested that the increment in arsenate removal percent was due to the existence of more adsorption sites as adsorbent dosage increases. Similar findings were reported by other researchers [35,43,44].

On the contrary, a significant decrease in arsenic uptake per HBC-RH mass unit was observed in Fig. 8, respectively. This could be attributed to the occurrence of abundant unsaturated active sites on HBC-RH during the sorption process. Prasanna Kumar et al. [45] linked the decrease in HBC-RH sorption efficiency to numerous factors such as high availability of sorbent, interference between active binding sites, electrostatic repulsion between surface charges and low mixing at high sorbent dose. These factors may render the binding sites unsaturated during sorption and consequently decreases the sorption efficiency of the sorbent.

### 3.7. Effect of initial concentration on arsenic removal

The initial sorbate concentration is a key parameter that has crucial influence on the removal of sorbates from solutions onto sorbents. Thus, the effect of initial arsenic concentration was determined by varying concentrations between 1 and  $150 \text{ mg L}^{-1}$ . But all other parameters remained unchanged ( $1 \text{ g L}^{-1}$  of HBC-RH dosage, pH of 6, and contact time of 48 h). Fig. 9 explicitly shows the effect of initial concentration on the sorption of arsenic.

The increase in arsenic concentration from 1 to  $100 \text{ mg L}^{-1}$  increases the amount of arsenic sorbed by HBC-RH from  $0.423$  to  $27.56 \text{ mg g}^{-1}$ . The amount of arsenic sorbed per mass unit of HBC-RH steadily increased as the initial concentration increases up to  $100 \text{ mg L}^{-1}$ . However, further increase in the initial arsenic concentration beyond  $100 \text{ mg L}^{-1}$  does not

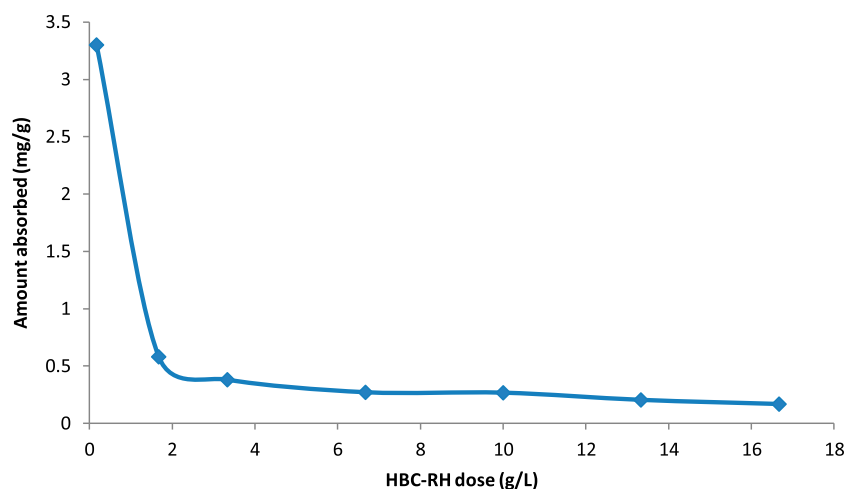


Fig. 8. Effect of HBC-RH dosage ( $\text{g L}^{-1}$ ) on the amount of arsenic uptake per sorbent mass unit (Arsenic:  $3 \text{ mg L}^{-1}$ , pH 6, 48 h, and  $28^\circ\text{C}$ ).

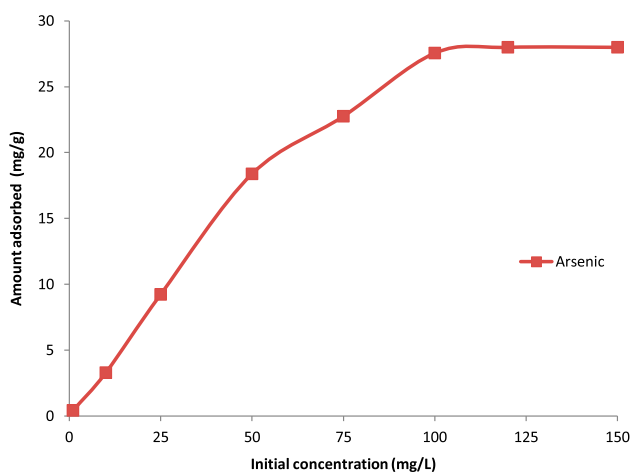


Fig. 9. Effect of initial concentration on the sorption of arsenic using HBC-RH (Arsenic:  $1 \text{ g L}^{-1}$  HBC-RH, pH 6, 48 h, and  $28^\circ\text{C}$ ).

reflect any significant uptake of arsenic onto HBC-RH. The graph in Fig. 9 illustrates that the amount of arsenic sorbed increases from 1 to  $100 \text{ mg L}^{-1}$  and eventually level-off from  $100$  to  $150 \text{ mg L}^{-1}$ . This plateau is considered as the equilibrium level. Equilibrium state is obtained when a point is reached at which the active sites of the sorbent are exhausted.

The increase in arsenic concentration gradient in solution was responsible for enhancing the sorption as the initial concentration increases. Concentration gradient is the driving force for mass transfer and it helps to surmount all possible mass transfer resistance. The effect of initial concentration has far-reaching influence on the sorption of arsenic using HBC-RH.

Nevertheless, it has little significance in the sorption of arsenic above the initial concentration threshold of  $100 \text{ mg L}^{-1}$ .

On the contrary, the gradual saturation of sorbent active sorption sites as the arsenic concentration gradient increase, eventually, decreases arsenic removal percentage from the aqueous medium. Thus, these results illustrate that arsenic sorption process using HBC-RH is more effective at lower initial metal concentrations. Barakat and Schmidt [46] had a similar conclusion regarding arsenate adsorption by anion exchange resin gel.

### 3.8. Effect of contact time on arsenic removal

The aim of investigating the effect of contact time on metal ion sorption was to determine the sorption rate of arsenic onto HBC-RH and the duration for the sorption process to reach equilibrium. A swift sorption of arsenic was observed (Fig. 10) within the first few hours of contact between the metal ion solution and HBC-RH. This was then followed by slower sorption rate until equilibrium was obtained. 94.85% of arsenic that was sorbed onto HBC-RH during the sorption process occurred within the first 6 h. Additional arsenic uptake of 4.92% was observed, when the contact time was extended to 24 h. Prolonging the contact time beyond 24 h, shows no further significant arsenic removal until an equilibrium state was obtained. The total time to reach equilibrium was about 48 h.  $0.447 \text{ mg g}^{-1}$  of arsenic was sorbed onto  $1 \text{ g L}^{-1}$  of HBC-RH with initial concentration of  $3 \text{ mg L}^{-1}$ .

The graphical representations of arsenic sorption as a function of time (in Figs. 13 and 14) are quite

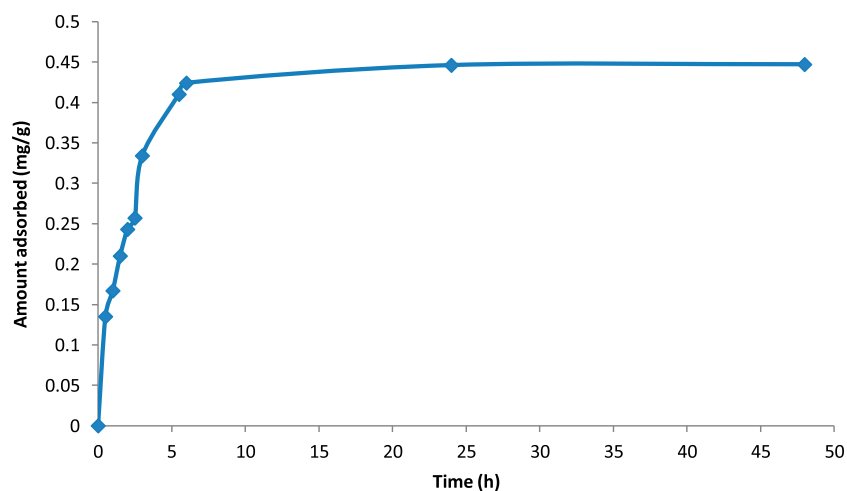


Fig. 10. Effect of contact time on the sorption of arsenic using HBC-RH (Arsenic.  $1 \text{ g L}^{-1}$  HBC-RH, pH 6,  $3 \text{ mg L}^{-1}$ , and  $28^\circ\text{C}$ ).

similar to the HBC-RH swelling behavior in Fig. 2. This can be attributed to the diffusion of arsenic ions along with the water into the HBC-RH. Pal et al. [47] reported that the diffusion of a solute (i.e. metal ions) into the hydrogel is influenced by the quantity of water imbibed within the hydrogel. Thus, the higher the  $S_{\text{eq}}\%$ , the higher the diffusion rate of metal ions through the HBC-RH. In other words, the sorption capacity of HBC-RH is influenced by the swelling of the composite. Kaşgöz [23] stated that low swelling degree of hydrogels affects their metal ion absorption capacities.

### 3.9. Sorption isotherm

This sorption isotherm study helps in predicting the arsenic sorption capacity of HBC-RH which is of paramount importance for the practical design of a sorption system. The experimental data acquired from the sorption of arsenic at different initial concentrations were utilized for the equilibrium isotherm studies. Though, many isotherm models exist but Langmuir and Freundlich model were employed to determine the sorption capacity of HBC-RH. Linear Langmuir isotherm graph of  $1/q_e$  vs.  $1/C_e$  was plotted (Fig. 11) while a graph of  $\log q_e$  vs.  $\log C_e$  was plotted

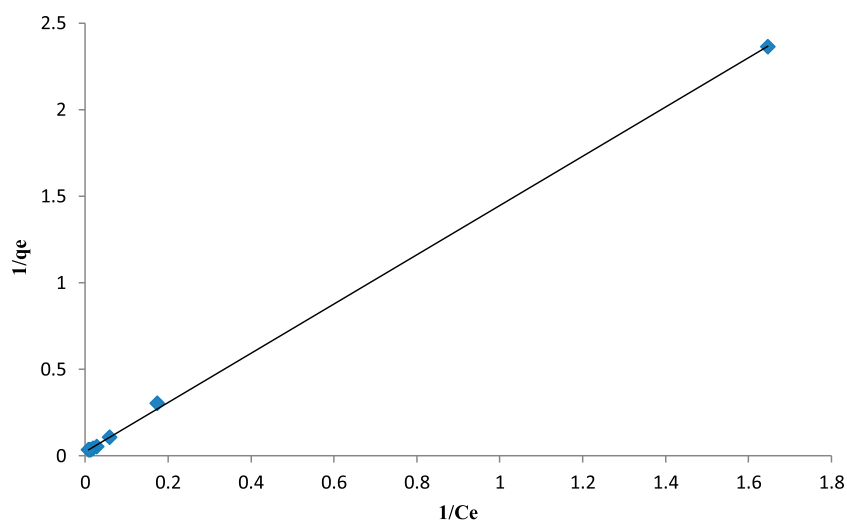


Fig. 11. Langmuir isotherm for the sorption of arsenic using HBC-RH.

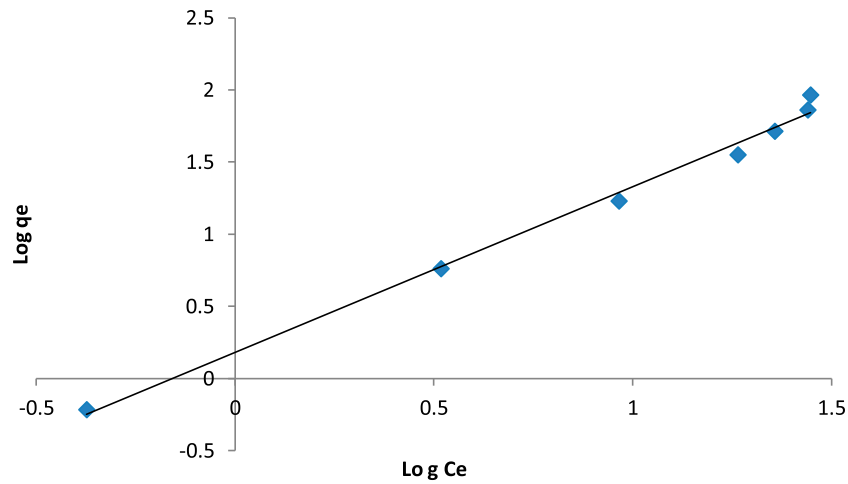


Fig. 12. Freundlich isotherm for the sorption of arsenic using HBC-RH.

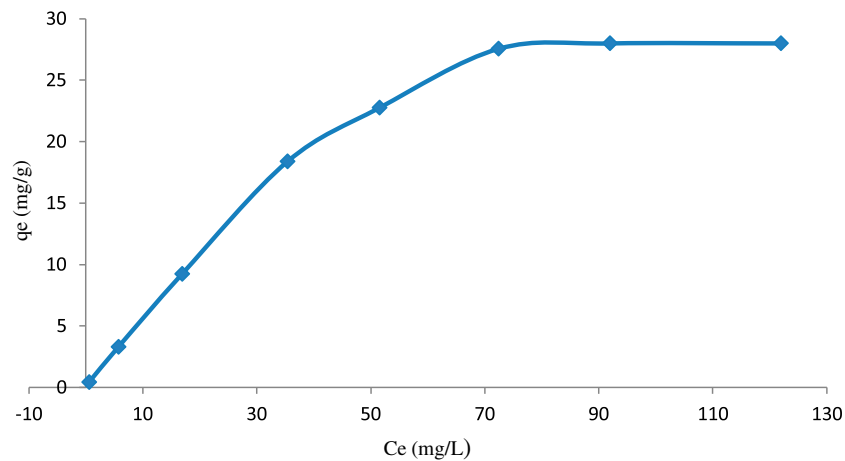


Fig. 13. The  $q_e$  vs.  $C_e$  graph for the sorption of arsenic at different concentrations.

for Freundlich isotherm (Fig. 12). Additionally, Fig. 13 shows arsenic isotherm equilibrium for HBC-RH. These plots indicate the milligram (mg) amount of arsenic on a gram (g) of HBC-RH sorbent ( $q$ ) against the remaining arsenic concentration in the solution ( $C_e$ ).

Table 1 presents the sorption constants and correlation coefficient ( $R^2$ ) of Langmuir and Freundlich model for arsenic. The  $R^2$  of Langmuir and Freundlich were 0.999 and 0.992 for arsenic, respectively. Comparison between the  $R^2$  of Langmuir and Freundlich isotherm for arsenic sorption manifested that Langmuir model best fitted arsenic experimental data than Freundlich. This indicates that HBC-RH sorption for arsenic was limited to monolayer sorption.

### 3.10. Sorption kinetics

In this study, pseudo-first-order and pseudo-second-order kinetic models were utilized for the evaluation of the sorption kinetics of arsenic onto HBC-RH. The rate of sorption in pseudo-first-order is

Table 1  
Comparison between Langmuir and Freundlich isotherm parameters

Contaminant	Langmuir isotherm parameters			Freundlich isotherm parameters		
	$K_L$	$q_{max}$	$R^2$	$K_F$	$n$	$R^2$
Arsenic	0.025	28.32	0.999	0.0091	0.871	0.992

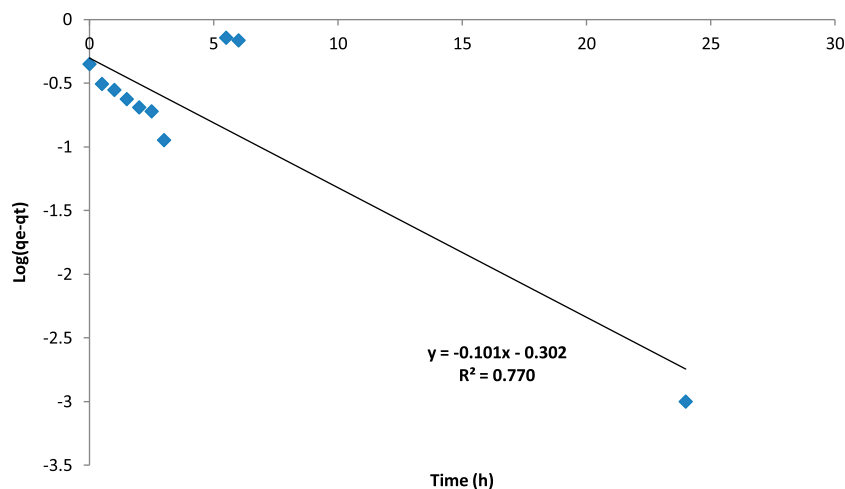


Fig. 14. Lagergrens first-order kinetics for the sorption of arsenic using HBC-RH.

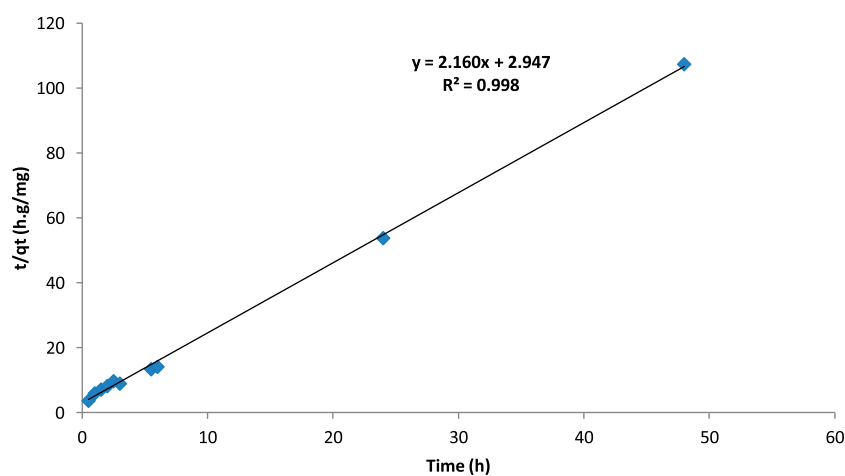


Fig. 15. Pseudo-second-order kinetics for the sorption of arsenic using HBC-RH.

proportional to the concentration gradient but proportional to the square of concentration gradient for the pseudo-second-order [48]. The experimental data for arsenic sorption rate onto HBC-RH were fitted into Eqs. (6) and (7).

The linearized plot of  $\log(q_e - q_t)$  vs.  $t$  and  $t/q_t$  vs.  $t$  for pseudo-first-order and pseudo-second-order are shown in Figs. 14 and 15, respectively. The sorption kinetic constants ( $k$ ) and the amount of metal ions sorbed at equilibrium ( $q_e$ ) in Table 2 were calculated from the slope and the intercept of the linear plot of both kinetic models. In addition, the correlation coefficient values ( $R^2$ ) in Table 2 were also determined from the linear graph of both models. The  $R^2$  and  $q_e$  are useful in identifying which of the two kinetic models

best fits the experimental data of the arsenic and zinc sorption.

The  $R^2$  of pseudo-first-order for arsenic sorption was low when compared with that of the pseudo-second-order kinetic model. This demonstrates that the pseudo-second-order best fitted the sorption of both contaminants onto HBC-RH than the pseudo-first-order model. Secondly, the calculated  $q_e$  for arsenic ( $0.463 \text{ mg g}^{-1}$ ) was closer to the experimental  $q_e$  which was  $0.447 \text{ mg g}^{-1}$ . Thus, suggesting that the sorption of arsenic using HBC-RH follows the pseudo-second-order kinetic model based on its high  $R^2$  and close proximity to the experimental  $q_e$ . Arsenic sorption been best fitted to the pseudo-second-order implies that the external and internal mass transfer are taking

Table 2  
Comparison between pseudo-first-order, pseudo-second-order, and experimental results

Contaminant	Pseudo-first-order			Pseudo-second-order			Experimental $q_e$ (mg g <sup>-1</sup> )
	$K_1$ (h <sup>-1</sup> )	$q_e$ (mg g <sup>-1</sup> )	$R^2$	$K_2$ (h <sup>-1</sup> )	$q_e$ (mg g <sup>-1</sup> )	$R^2$	
Arsenic	0.233	0.499	0.77	1.581	0.463	0.998	0.447

Table 3  
Comparison of sorption capacity of different sorbent for the removal of arsenic

Sorbent	Initial concentration (mg L <sup>-1</sup> )	Sorption capacity (mg g <sup>-1</sup> )	References
Pine wood char	0.1	1.20	[34]
Oak wood char		5.85	
Pine bark char		12.15	
Oak bark char		7.40	
Iron- chitosan	1.007	6.82	[52]
<b>HBC-RH</b>	<b>1–150</b>	<b>28.32</b>	Present study

Note: The sorbent and values in bold shows the results of the current study compared to previous studies.

place and that sorption may be the rate limiting step [49,50].

### 3.11. Sorption capacity: HBC-RH compared with other adsorbents

Sorption capacity of HBC-RH and other adsorbents for the removal of arsenic has been compared in Table 3, which is only a tentative comparison due to variation in parameters and experimental conditions. The comparison was to justify the validity of HBC-RH as a promising hybrid sorbent for the sorption of arsenic from aqueous media. HBC-RH manifested a considerable higher arsenic sorption capacity than the other adsorbents listed in Table 3. The variations in sorption capacity of different adsorbents for metal ions uptake are attributed to numerous factors, primarily adsorbent surface area, porosity, and functional groups [51].

## 4. Conclusions

HBC-RH was successfully synthesized and its equilibrium swelling percentage ( $S_{eq}\%$ ) was 1,008% which is comparable or better than most hydrogel or hydrogel composites in literatures. The high swelling performance of HBC-RH was attributed to the presence of several hydrophilic functional groups on HBC-RH. HBC-RH sorption of arsenic was significantly influenced by changing the solution pH and the optimum pH value obtained was 6. The increase in

HBC-RH dosage from 0.167 to 16.67 g L<sup>-1</sup> resulted to a considerable increase in arsenic removal from 18.35 to 93%. The removal of arsenic increased as more HBC-RH was loaded into the solutions. On the contrary, a decrease in arsenic uptake per mass unit of HBC-RH was observed as HBC-RH dosage increased. Varying the initial concentration of arsenic from 1 to 150 mg L<sup>-1</sup>, increases the equilibrium sorption capacity of HBC-RH from 0.42 to 27.56 mg g<sup>-1</sup>. However, a decrease in removal percentage was realized as the initial contaminant concentration increases. Almost 95% of arsenic adsorbed by HBC-RH occurred within the initial 6 h which was later followed by slower sorption rate until equilibrium was achieved after 48 h of constant agitation. The isotherm and kinetic models were best described by Langmuir isotherm and pseudo-second-order kinetic model. The latter indicates that the chemisorption mechanism is the rate limiting step in the sorption uptake. This investigation manifested that HBC-RH has a promising potential for the effective removal of arsenic from aqueous media.

## Acknowledgements

The authors express their gratitude to the Ministry of Science, Technology and Innovation (MOSTI) of Malaysia, Academy Science of Malaysia and Ministry of Higher Education (MOHE) of Malaysia (FRGS 03-0104-799FR/5523839) for financial support.

## References

- [1] P. Smedley, D. Kinniburgh, A review of the source, behaviour and distribution of arsenic in natural waters, *Appl. Geochem.* 17 (2002) 517–568.
- [2] B.K. Biswas, J. Inoue, K. Inoue, K.N. Ghimire, H. Harada, K. Ohto, H. Kawakita, Adsorptive removal of As(V) and As(III) from water by a Zr(IV)-loaded orange waste gel, *J. Hazard. Mater.* 154 (2008) 1066–1074.
- [3] J.O. Duruibe, M.O.C. Ogwuegbu, J.N. Egwurugwu, Heavy metal pollution and human biotoxic effects, *Int. J. Phys. Sci.* 2 (2007) 112–118.
- [4] C.K. Jain, I. Ali, Arsenic: Occurrence, toxicity and speciation techniques, *Water Res.* 34 (2000) 4304–4312.
- [5] USEPA, Arsenic Treatment Technology Evaluation Handbook for Small System, EPA 816-R-03-014, USEPA, Washington, DC, 2000.
- [6] C. Hopenhayn-Rich, M. Lou Biggs, A. Fuchs, R. Bergoglio, E.E. Tello, H. Nicolli, A.H. Smith, Bladder cancer mortality associated with arsenic in drinking water in Argentina. *Epidemiology* 7 (1996) 117–124.
- [7] M. Goyal, V.K. Rattan, D. Aggarwal, R.C. Bansal, Removal of copper from aqueous solutions by adsorption on activated carbons, *Colloids Surf., A* 190 (2001) 229–238.
- [8] T. Aman, A.A. Kazi, M.U. Sabri, Q. Bano, Potato peels as solid waste for the removal of heavy metal copper (II) from waste water/industrial effluent, *Colloids Surf., B* 63 (2008) 116–121.
- [9] E.-S. El-Ashtoukhy, N.K. Amin, O. Abdelwahab, Removal of lead (II) and copper (II) from aqueous solution using pomegranate peel as a new adsorbent, *Desalination* 223 (2008) 162–173.
- [10] W. Zheng, X. Li, F. Wang, Q. Yang, P. Deng, G. Zeng, Adsorption removal of cadmium and copper from aqueous solution by areca—A food waste, *J. Hazard. Mater.* 157 (2008) 490–495.
- [11] A. Bhatnagar, M. Sillanpää, Utilization of agro-industrial and municipal waste materials as potential adsorbents for water treatment—A review, *Chem. Eng. J.* 157 (2010) 277–296.
- [12] F. Fu, Q. Wang, Removal of heavy metal ions from wastewaters: A review, *J. Environ. Manage.* 92 (2011) 407–418.
- [13] M.A. Barakat, New trends in removing heavy metals from industrial wastewater, *Arab. J. Chem.* 4 (2011) 361–377.
- [14] C.L. Chuang, M. Fan, M. Xu, R.C. Brown, S. Sung, B. Saha, C.P. Huang, Adsorption of arsenic(V) by activated carbon prepared from oat hulls, *Chemosphere* 61 (2005) 478–483.
- [15] S. Chakraborty, M. Wolthers, D. Chatterjee, L. Charlet, Adsorption of arsenite and arsenate onto muscovite and biotite mica, *J. Colloid Interface Sci.* 309 (2007) 392–401.
- [16] H. Guo, D. Stüben, Z. Berner, Adsorption of arsenic (III) and arsenic(V) from groundwater using natural siderite as the adsorbent, *J. Colloid Interface Sci.* 315 (2007) 47–53.
- [17] D. Mohapatra, D. Mishra, K.H. Park, A laboratory scale study on arsenic(V) removal from aqueous medium using calcined bauxite ore, *J. Environ. Sci. (China)* 20 (2008) 683–689.
- [18] Y. Tian, M. Wu, X. Lin, P. Huang, Y. Huang, Synthesis of magnetic wheat straw for arsenic adsorption, *J. Hazard. Mater.* 193 (2011) 10–16.
- [19] A. Goswami, P.K. Raul, M.K. Purkait, Arsenic adsorption using copper (II) oxide nanoparticles, *Chem. Eng. Res. Des.* 90 (2012) 1387–1396.
- [20] T.G. Chuah, A. Jumariah, I. Azni, S. Katayon, S.Y. Thomas Choong, Rice husk as a potentially low-cost biosorbent for heavy metal and dye removal: An overview, *Desalination* 175 (2005) 305–316.
- [21] S. Noor Syuhadah, H. Rohasliney, Rice husk as biosorbent: A review, *Health Environ. J.* 3 (2012) 89–95.
- [22] H. Kaşgöz, S. Özgümüş, M. Orbay, Modified polyacrylamide hydrogels and their application in removal of heavy metal ions, *Polymer* 44 (2003) 1785–1793.
- [23] H. Kaşgöz, New sorbent hydrogels for removal of acidic dyes and metal ions from aqueous solutions, *Polym. Bull.* 56 (2006) 517–528.
- [24] O. Ozay, S. Ekici, Y. Baran, N. Aktas, N. Sahiner, Removal of toxic metal ions with magnetic hydrogels, *Water Res.* 43 (2009) 4403–4411.
- [25] B.L. Rivas, C. Muñoz, Functional water-insoluble polymers with ability to remove arsenic(V), *Polym. Bull.* 65 (2009) 1–11.
- [26] B.L. Rivas, I.M. Perič, C. Muñoz, R. Alvear, Poly(N-hydroxymethyl acrylamide-co-acrylic acid) and poly(N-hydroxymethyl acrylamide-co-acrylamidoglycolic acid): Synthesis, characterization, and metal ion removal properties, *Polym. Bull.* 68 (2011) 391–403.
- [27] P. Chutia, S. Kato, T. Kojima, S. Satokawa, Adsorption of As(V) on surfactant-modified natural zeolites, *J. Hazard. Mater.* 162 (2009) 204–211.
- [28] N. Karakoyun, S. Kubilay, N. Aktas, O. Turhan, M. Kasimoglu, S. Yilmaz, N. Sahiner, Hydrogel-biochar composites for effective organic contaminant removal from aqueous media, *Desalination* 280 (2011) 319–325.
- [29] E.-S. El-Ashtoukhy, N.K. Amin, O. Abdelwahab, Removal of lead (II) and copper (II) from aqueous solution using pomegranate peel as a new adsorbent, *Desalination* 223 (2008) 162–173.
- [30] F.-M. Pellerá, A. Giannis, D. Kalderis, K. Anastasiadou, R. Stegmann, J.-Y. Wang, E. Gidaracos, Adsorption of Cu(II) ions from aqueous solutions on biochars prepared from agricultural by-products, *J. Environ. Manage.* 96 (2012) 35–42.
- [31] Y. Yao, B. Gao, H. Chen, L. Jiang, M. Inyang, A.R. Zimmerman, X. Cao, L. Yang, Y. Xue, H. Li, Adsorption of sulfamethoxazole on biochar and its impact on reclaimed water irrigation, *J. Hazard. Mater.* 209–210 (2012) 408–413.
- [32] M.A. Barakat, N. Sahiner, Cationic hydrogels for toxic arsenate removal from aqueous environment, *J. Environ. Manage.* 88 (2008) 955–961.
- [33] O. Ozay, S. Ekici, Y. Baran, S. Kubilay, N. Aktas, N. Sahiner, Utilization of magnetic hydrogels in the separation of toxic metal ions from aqueous environments, *Desalination* 260 (2010) 57–64.
- [34] D. Mohan, C.U. Pittman Jr, M. Bricka, F. Smith, B. Yancey, J. Mohammad, P.H. Steele, M.F. Alexandre-Franco, V. Gómez-Serrano, H. Gong, Sorption of arsenic, cadmium, and lead by chars produced from fast pyrolysis of wood and bark during bio-oil production, *J. Colloid Interface Sci.* 310 (2007) 57–73.

- [35] D. Vasireddy, Arsenic adsorption onto iron-chitosan composite from drinking water, Doctoral dissertation, University of Missouri, 2006.
- [36] N.A. Peppas, P. Bures, W. Leobandung, H. Ichikawa, Hydrogels in pharmaceutical formulations, *Eur. J. Pharm. Biopharm.* 50 (2000) 27–46.
- [37] Y. Mamindy-Pajany, C. Hurel, N. Marmier, M. Roméo, Arsenic (V) adsorption from aqueous solution onto goethite, hematite, magnetite and zero-valent iron: Effects of pH, concentration and reversibility, *Desalination* 281 (2011) 93–99.
- [38] D. Tiwari, S.M. Lee, Novel hybrid materials in the remediation of ground waters contaminated with As (III) and As(V), *Chem. Eng. J.* 204–206 (2012) 23–31.
- [39] J.S. Vani, K.M. Rao, N.S.G. Reddy, K.S.V.K. Rao, Synthesis and characterization of sodium carboxy methyl cellulose/poly (acrylamide) magnetic nano composite semi Ipn 's for removal of heavy metal ions, *World J. Chem.* 2 (2013) 33–41.
- [40] M. Ahmaruzzaman, Industrial wastes as low-cost potential adsorbents for the treatment of wastewater laden with heavy metals, *Adv. Colloid Interface Sci.* 166 (2011) 36–59.
- [41] B. Manna, U.C. Ghosh, Adsorption of arsenic from aqueous solution on synthetic hydrous stannic oxide, *J. Hazard. Mater.* 144 (2007) 522–531.
- [42] Y.-N. Chen, L.-Y. Chai, Y.-D. Shu, Study of arsenic(V) adsorption on bone char from aqueous solution, *J. Hazard. Mater.* 160 (2008) 168–172.
- [43] Y.-S. Ho, Removal of copper ions from aqueous solution by tree fern, *Water Res.* 37 (2003) 323–2330.
- [44] Y.-T. Wei, Y.-M. Zheng, J.P. Chen, Uptake of methylated arsenic by a polymeric adsorbent: Process performance and adsorption chemistry, *Water Res.* 45 (2011) 2290–2296.
- [45] Y. Prasanna Kumar, P. King, V.S.R.K. Prasad, Adsorption of zinc from aqueous solution using marine green algae—*Ulva fasciata* sp, *Chem. Eng. J.* 129 (2007) 161–166.
- [46] M.A. Barakat, E. Schmidt, Polymer-enhanced ultrafiltration process for heavy metals removal from industrial wastewater, *Desalination* 256 (2010) 90–93.
- [47] K. Pal, A.K. Banthia, D.K. Majumdar, Polymeric hydrogels: Characterization and biomedical applications, *Des. monomers Polym.* 12 (2009) 197–220.
- [48] M.A. Malana, R.B. Qureshi, M.N. Ashiq, Adsorption studies of arsenic on nano aluminium doped manganese copper ferrite polymer (MA, VA, AA) composite: Kinetics and mechanism, *Chem. Eng. J.* 172 (2011) 721–727.
- [49] R. Rakhshae, M. Khosravi, M.T. Ganji, Kinetic modeling and thermodynamic study to remove Pb(II), Cd(II), Ni(II) and Zn(II) from aqueous solution using dead and living *Azolla filiculoides*, *J. Hazard. Mater.* 134 (2006) 120–129.
- [50] B. Özkahraman, I. Acar, K. Güçlü, G. Güçlü, Synthesis of Zn(II) ion-imprinted polymeric adsorbent for selective removal of zinc from aqueous solutions, *Polym. Plast. Technol. Eng.* 50 (2011) 216–219.
- [51] X.-S. Wang, Y. Qin, Removal of Ni(II), Zn(II) and Cr(VI) from aqueous solution by *Alternanthera philoxeroides* biomass, *Journal of Hazardous Materials* 138 (2006) 582–588.
- [52] D.D. Gang, B. Deng, L. Lin, As(III) removal using an iron-impregnated chitosan sorbent, *J. Hazard. Mater.* 182 (2010) 156–161.